Journal of Innovative Optical Health Sciences
Vol. 11, No. 2 (2018) 1750013 (7 pages)

DOI: 10.1142/S1793545817500134

World Scientific
www.worldscientific.com

Scanless multitarget-matching multiphoton excitation fluorescence microscopy

Junpeng Qiu*, Lei Wang*, Bruce Zhi Gao†, Junle Qu*,§ and Yonghong Shao*,‡,§
*College of Optoelectronics Engineering
Key Laboratory of Optoelectronic Devices and Systems of Ministry
of Education and Guangdong Province
Shenzhen University, Shenzhen 518060, P. R. China
†Department of Bioengineering and COMSET
Clemson University, Clemson, SC 29634, USA
‡shaoyh@gzu.edu.cn

Received 06 November 2016
Accepted 05 March 2017
Published 14 April 2017

Using the combination of a reflective blazed grating and a reflective phase-only diffractive spatial light modulator (SLM), scanless multitarget-matching multiphoton excitation fluorescence microscopy (SMTM-MPM) was achieved. The SLM shaped an incoming mode-locked, near-infrared Ti:sapphire laser beam into an excitation pattern with addressable shapes and sizes that matched the samples of interest in the field of view. Temporal and spatial focusing were simultaneously realized by combining an objective lens and a blazed grating. The fluorescence signal from illuminated areas was recorded by a two-dimensional sCMOS camera. Compared with a conventional temporal focusing multiphoton microscope, our microscope achieved effective use of the laser power and decreased photodamage with higher axial resolution.

Keywords: Multitarget-matching; multiphoton microscopy; SLM; temporal focusing.

1. Introduction

Multiphoton excited fluorescence microscopy has become an important tool in the field of biomedical optical imaging.[1–3] It is widely used in biomedical detection because nonlinear excitation of the near-infrared femtosecond laser delivers low damage, a large depth of penetration in highly scattered tissues and high axial resolution with no confocal aperture.[4–7] As traditional multiphoton microscopy is based on single excitation beam scanning, imaging speed and the inflexible scanning method limit its applications in some important biological imaging processes. For example, in the study of cardiomyocyte interaction with stem cells,[8] to avoid photodamage to cardiomyocytes during rapid imaging of the stem cell dynamic process, selective

§Corresponding authors.

excitation of stem cells is required; in the study of cellular and cellular communication in the neural networks, it is necessary only to select the excitation of the cells of interest. In these applications, the rapid speed multiphoton microscopy with the capability of target-selective excitation imaging is required. In general life science research, target-selective excitation multiphoton microscopy has obvious advantages: it is possible to avoid sample damage outside the target area of interest in the study of cellular interactions. To improve imaging speed, electrical scanning technologies such as galvanometer scanning and resonance mirror scanning have been developed, and many types of fast excitation methods to increase imaging speed have been developed.[9–15] Multifocal multiphoton microscopy (MMM) was reported by Hell's group in 1998.[11] The laser's full power is distributed into multiple beamlets that are focused to form a multifocal array. At each focal point, multiphoton fluorescence is generated with appropriate peak power. Each beamlet is required to scan only a sub-region, and the entire field of view (FOV) is scanned in parallel by the multifocal array so that the imaging speed is approximately equal to the original single-beam rate multiplied by the number of beamlets. Several practical MMM techniques involving microlens array,[16] cascaded splitter,[17] diffractive optical element (DOE),[12] spatial light modulator (SLM)[18,19] and the Nipkow disk[11] have been widely reported. To further improve imaging speed, Chris Xu's group proposed and developed the temporal focusing multiphoton microscope (TF-MPM) in 2005.[20] Excitation light disperses into different diffraction angles at different frequencies using a reflective blazed grating then goes through a tube lens and an objective lens and focuses at the back focal plane of the objective lens. At the focal plane, the shortest pulse width and strongest peak power are produced. The laser pulse width increases rapidly as the distance from the focal plane of the objective lens increases, and peak power decreases rapidly. Therefore, the conditions of two-photon excitation can be met only in the focal plane of the objective lens in which wide-field two-photon imaging can be realized. Recently, a variety of TF-MPM methods based on dispersive elements, such as an optical diffuser;[21] a combination of two prisms and a grating;[22] and a digital micromirror device[23] have been developed.

However, the techniques described above cannot obtain the image of only particular samples of interest in the FOV because the excitation light on the grating surface is a uniform light spot, which will generate a uniform excitation light spot to illuminate the whole FOV. This illumination method does not permit selectively excitation of specific samples. To develop the selective target multiphoton microscopy, several techniques have been reported. Saggau's group developed jump scanning imaging of the point of interest using two-dimensional acousto-optic deflectors (2D AODs) to avoid photodamage to the other points.[24] Shao *et al.* reported addressable multiregional and multifocal multiphoton microscopy using multifocal excitation pattern matching of samples of interest.[16] However, using this microscope, the scanned area does not accurately match the sample of interest because each focal point scans the same distance. Glückstad's group reported shape illumination microscopy by combining the raster generalized phase contrast (GPC) technique with a grating.[25,26] In the present study, we developed a scanless multitarget-matching multiphoton excited fluorescence microscopy (SMTM-MPM). The temporal focusing on any areas in the FOV was realized by combining an SLM and a blazed grating. The SLM modulated the incident light to produce a target pattern matching the samples of interest in the FOV. The blazed grating dispersed the incident light pattern with different frequencies at different angles. The dispersed light re-generated the excitation pattern in the sample through a tube lens and objective lens. The excitation pattern has the narrowest pulse width at the focal plane of the objective lens, and the pulse width dramatically stretched as the distance from the focal plane increased. Experimental results showed that an axial resolution of 2.2 μm was achieved.

2. Experimental Setup

Figure 1 shows a schematic of our experimental setup based on SLM and grating. A mode-locked Ti: sapphire laser (Coherent, Chameleon Ultra II) was tuned at a wavelength of 800 nm and a pulse duration of 100 fs. The maximum output power was 3.5 W. The laser beam from a mode-locked Ti:sapphire laser was expanded and collimated to slightly overfill the phase-only SLM (Holoeye Pluto, NIR, 1920 $\times$ 1080 pixels, eight bits), which was capable of completing 2π phase modulation at each pixel with

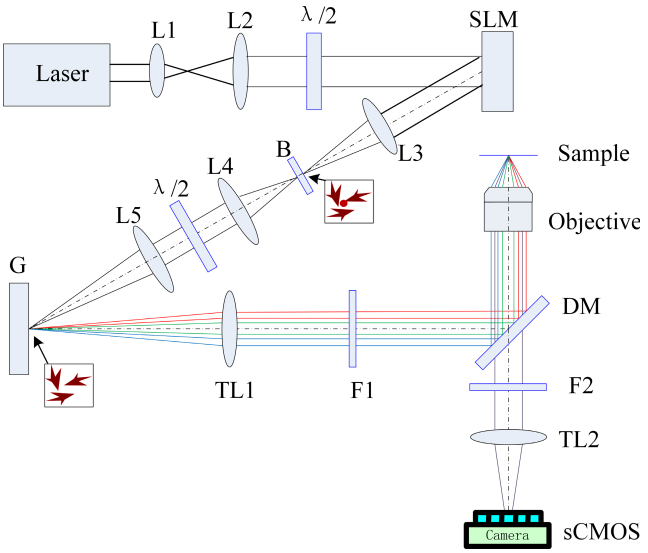

Fig. 1. Schematic of our SMTM-MPM based on the combination of a SLM and grating. The grating, TL1 and the objective lens comprise a temporal focusing system. The SLM on the back focal plane of Fourier lens L3 modulates the input fs beam to generate the required excitation pattern matching the target sample of interest on the front focal plane of L3. The zero-order light is blocked by a blocker. The polarization of the fs beam is tuned by a $\lambda/2$ wave plate. Laser: a model-locked laser that generates an fs beam; L1 to 5: lens; B: blocker; TL1 and TL2: tube lens; F: filter; DM: dichroic mirror; Camera: sCMOS camera.

a 60 Hz refresh rate. To improve the diffraction efficiency of the SLM and grating, a $\lambda/2$ wave plate was included to tune the polarization of incident light before the SLM and grating, respectively. The SLM can be used to dynamically produce arbitrary patterns with computer-generated phase-only holograms based on the required excitation pattern. An accurate phase pattern can be generated by employing phase retrieval algorithms such as the classic Gerchberg–Saxton algorithm[27] or by directly utilizing the Holoeye application software. A Fourier lens with a focal length of 200 mm transferred the light that was phase-modulated by the SLM into an arbitrary pattern. The pattern matched the samples of interest at the back focal plane, at which a spatial filter was used to block the unwanted zero order created by the SLM. The largest illumination pattern was about 15 mm, approximately the size of the microscope's FOV at the back focal plane of the tube lens. A pair of 1:1 relay lenses was used to transfer the illumination pattern to an 800 l/mm reflective grating located at the back focal plane of the tube lens, the front focal plane of which was located at the entrance of the microscope objective. The reflective grating, tube lens and objective constitute a typical temporal focusing system. The objective (Nikon 100×) then produced an illumination pattern matching the target samples at the sample plane. Thus, only the samples at the focusing plane were excited. The corresponding fluorescence signals from the samples were recorded by a sCMOS camera (Andor, Zyla 5.5).

In our experiment, the process of microscopy imaging mainly included the following five steps: (1) Obtain a white light wide-field image in the white light illumination mode. (2) Extract the position and boundary of the samples of interest based on the above white light image. (3) Calculate the phase-hologram of the illumination pattern using Holoeye application software based on the parameters obtained in step 2. (4) Modulate the excitation light to generate the target-sample-matching illumination pattern by uploading the phase-hologram to SLM. (5) Record the two photon excited fluorescence signals using a 2D sCMOS camera.

3. Results and Discussion

3.1. *Analysis of the performance of our microscopy*

To prove any pattern excitation capability without scanning the excitation light, we designed an excitation light pattern in the objective plane of the objective lens consisting of four different shapes (Fig. 2(a)), in which white areas are light and black areas are no light. The size of the pattern was $150 \times 150\,\mu$m to match the size of the FOV. The required phase-hologram was calculated using Holoeye application software based on the size of the amplified pattern at a magnification of 100×. A 15×15 mm excitation light pattern was generated on the reflecting surface of the blaze grating. The temporal focusing system consisted of a tube lens and objective lens which executed temporal focusing to simultaneously excite the target samples of interest selected in wide field illumination for each sub-region spot. Rhodamine (5%) was selected as a sample and the exposure time was 100 ms. The two-photon image, shown in Fig. 2(b), consisted of four different shapes obtained by the sCMOS camera with no scanning of the excitation light beam.

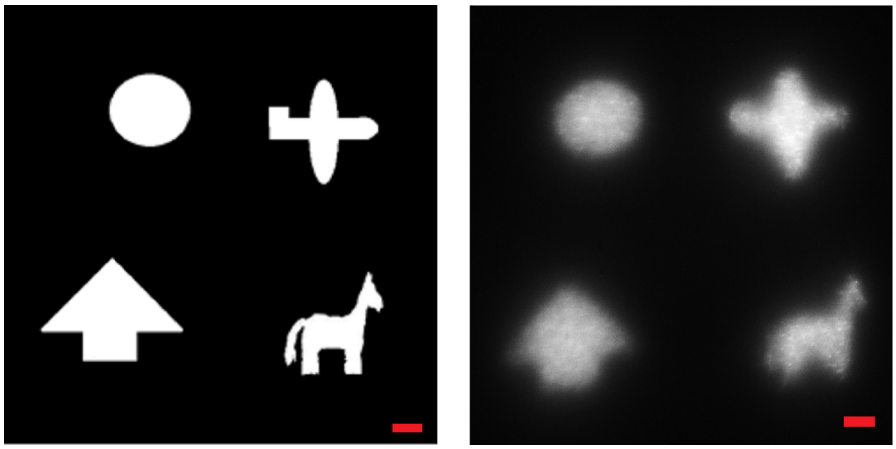

(a) (b)

Fig. 2. The process of imaging the arbitrary shapes of the samples. (a) The required excitation light pattern including four different shapes and (b) the two-photon fluorescence image of 5% rhodamine solution excited by the required excitation light pattern. Scale bar is 10 μm.

3.2. *Imaging of pollen grains and dyed cells*

The spatial resolution of our microscopy system was examined and compared with that of traditional TF-MPM using an 800 nm laser beam with an average power of 1.6 W at the back entrance of the objective lens. In Fig. 3, the z-axis shows the distribution of the fluorescence intensity in the beam center obtained by scanning a 0.19 μm fluorescent bead using our system and traditional TF-MPM, respectively. From the data obtained, the axial resolutions of our system and traditional TF-MPM were estimated using a deconvolution procedure[28]

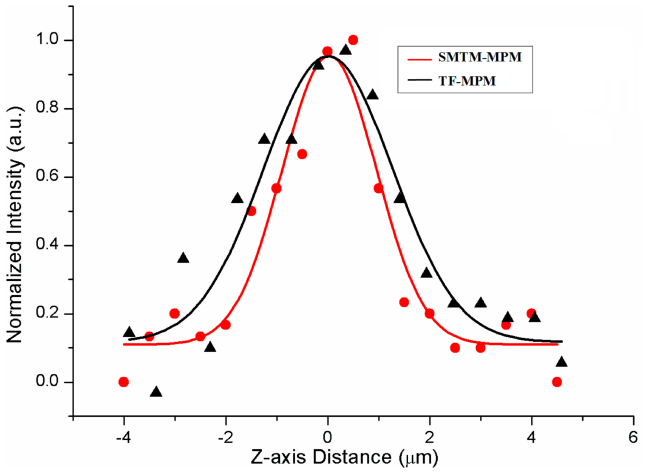

Fig. 3. The fluorescence-intensity profile obtained by scanning a 0.19 μm fluorescence bead along the z-axis using (a) our SMTM-MPM (red) and (b) TF-MPM (black).

to be 2.2 and 2.8 μm, respectively. To assess image quality, the Convallaria rhizome images obtained by the traditional TF-MPM and our system, respectively, are shown in Fig. 4. These results show that our system had higher z-axial resolution than traditional TF-MPM. Compared to the parallel beam in traditional TF-MPM, the convergent beam in our system increasingly expanded as the distance from the focal plane of the objective lens increased.

To demonstrate the matching ability of our SMTM-MPM in imaging biological samples, we imaged fresh pollen grains. First, we changed the optical path to the white light illumination mode. The white light image of flower pollen grains in the whole FOV was obtained by the sCMOS camera, and the outlines of the selected cells were distinguished through the image edge detection algorithm based on a canny operator, as shown in Fig. 5(a). The positions and boundary profiles of target samples were extracted using our homemade algorithms, as marked by the red curve in Fig. 5(a). The corresponding excitation light pattern in the objective plane of the objective lens is shown in Fig. 5(b). By uploading the calculated phase-hologram to the SLM, the required excitation pattern matching the target samples was then produced through SLM modulating incident light (Fig. 5(b)), in which the white areas are excitation light and the black areas are no light. The total +1 order diffraction light power of incident light at the microscope objective entrance pupil was approximately 1.6 W. Because only the first order of diffraction was used, the

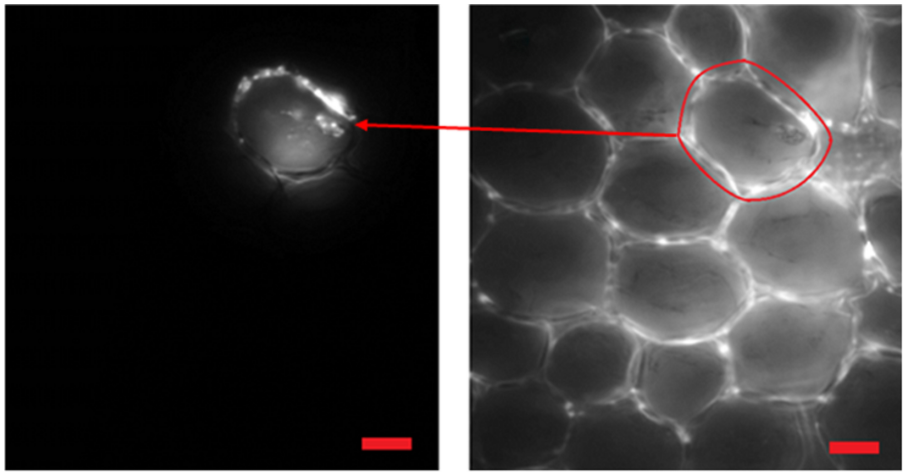

(a) (b)

Fig. 4. Two photon fluorescence images of a Convallaria rhizome slide obtained by (a) our system and (b) a traditional TF-MPM. Scale bar is 10 μm.

(a) (b) (c)

Fig. 5. The process of imaging pollen grains of interest. (a) The white light image of pollen grains in the wide field mode in which the boundary of samples of interest is marked by the red curve; (b) the required excitation light pattern matching the samples of interest and (c) the two-photon fluorescence image of pollen grains of interest. Scale bar is 10 μm.

(a) (b) (c)

Fig. 6. The process of imaging dyed cells of interest. (a) the white light image of cells in the wide field mode in which the boundary of the samples of interest is marked by the red curve; (b) the required excitation light pattern matching the samples of interest and (c) the two-photon fluorescence image of dyed cells of interest. Scale bar is 10 μm.

unwanted zero order created by the SLM was blocked by a spatial filter. The light efficiency of the microscopy light path before the objective was approximately 53%. The exposure time of the sCMOS camera was about 10 s. The two-photon fluorescence image of the target pollen grains obtained by the sCMOS camera is shown in Fig. 5(c). The excitation pattern matched the target pollen grains well. In addition, we also obtained the two-photon fluorescence image of the dyed cells using our microscopy. Figure 6(a) shows the white light image of the rhodamine 123 dye-labeled cells, among which the cells labeled in 1, 2 and 3 are the target cells of interest. We extracted the position, shape and size of the target cells and then calculated the corresponding phase-hologram of the excitation light pattern shown in Fig. 6(b). The excitation light pattern was produced by SLM modulating the incident light. The exposure time of the sCMOS camera was 30 s to improve the signal-to-noise ratio of the two-photon fluorescence image. The two-photon image of the target cells is shown in Fig. 6(c).

4. Conclusion

We developed novel multitarget-matching multiphoton excitation fluorescence microscopy by combining SLM and a grating. SLM can produce any light pattern by uploading the corresponding phase-hologram without changing the light path or scanning the light beam. The combination of grating with objective lens managed the dispersion characteristics of the femtosecond pulse laser. The temporal focusing of the pulse laser was realized only at the objective plane of the objective lens and ensured wide-field two-photon fluorescence imaging without compromising spatial resolution. Compared to traditional wide-field TF-MPM based on the parallel beam of the incident light on the grating, our SMTM-MPM with the converging beam of incident light on the grating had higher axial resolution. The main reason for this is that convergence of the beam had a faster power density change along the z-axial distance out of the focal plane of the objective lens. In our experiments, the speed of imaging was not as fast as expected. This may have been due to the low signal-to-noise ratio of the sCMOS camera. Because our sCMOS dark current of 0.14 e/s is 100 times greater than the EMCCD dark current of 0.001 e/s per pixel, we will replace the sCMOS camera with an EMCCD camera in the future.

In conclusion, we report multitarget-matching multiphoton excitation fluorescence microscopy, which simultaneously produced the required matching excitation pattern and imaged multiple target samples of interest without scanning. This method improved the efficiency of laser power use, maintained high spatial and temporal resolution and decreased photodamage to samples. This method has great potential in studying the interactions of cells and dynamic biological processes.

Acknowledgments

This work has been partially supported by Specially Funded Program on National Key Scientific Instruments and Equipment Development (61527827), Program 973 (2015CB352005); the National Natural Science Foundation of China (31171372/61525503/61378091/61620106016), Guangdong Natural Science Foundation (2014A030312008/2015A020214023/2015KGJHZ002), Shenzhen Science and Technology R&D Foundation (JCYJ20160422151611496).

References

1. V. E. Centonze, J. G. White, "Multiphoton excitation provides optical sections from deeper within scattering specimens than confocal imaging," *Biophys. J.* **75**(4), 2015 (1998).
2. W. Denk, J. H. Strickler, W. W. Webb, "2-Photon Laser Scanning Fluorescence Microscopy," *Science* **248**(4951), 73 (1990).
3. A. H. Buist *et al.*, "Real time two-photon absorption microscopy using multi point excitation," *J. Microsc.* **192**(2), 217 (1998).
4. A. V. Kachynski, A. Pliss, A. N. Kuzmin, T. Y. Ohulchanskyy, A. Baev, J. Qu, P. N. Prasad, "Photodynamic therapy by in situ nonlinear photon conversion," *Nature Photon.* **8**, 455 (2014).
5. W. R. Zipfel, R. M. Williams, W. W. Webb, "Nonlinear magic: Multiphoton microscopy in the biosciences," *Nat. Biotechnol.* **21**, 1369 (2003).
6. A. Vogel, J. Noack, G. Hüttman, G. Paltauf, "Mechanisms of femtosecond laser nanosurgery of cells and tissues," *Appl. Phys. B* **81**, 1015 (2005).
7. H. Liu, Y. Shao, W. Qin, R. B. Runyan, M. Xu, Z. Ma, T. K. Borg, R. Markwald, B. Z. Gao, "Myosin filament assembly onto myofibrils in live neonatal cardiomyocytes observed by TPEF-SHG microscopy," *Cardiovasc. Res.* **97**, 262 (2013).

8. Z. Ma, Q. Liu, H. Liu, H. Yang, J. X. Yun, C. Eisenberg, T. K. Borg, M. Xu, B. Z. Gao, "Laser-patterned stem-cell bridges in a cardiac muscle model for on-chip electrical conductivity analyses," *Lab Chip* **12**, 566 (2012).
9. J. D. Lechleiter, D. T. Lin, I. Sieneart, "Multiphoton laser scanning microscopy using an acoustic optical deflector," *Biophys. J.* **83**, 2292 (2002).
10. N. Ji, J. C. Magee, E. Betzig, "High-speed, low-photodamage nonlinear imaging using passive pulse splitters," *Nat. Methods* **5**, 197 (2008).
11. J. Bewersdorf, R. Pick, S. W. Hell, "Multifocal multiphoton microscopy," *Opt. Lett.* **23**(9), 655 (1998).
12. J. E. Jureller, H. Y. Kim, N. F. Scherer, "Stochastic scanning multiphoton multifocal microscopy," *Opt. Express* **14**(8), 3406 (2006).
13. V. Nikolenko *et al.*, "SLM microscopy: Scanless two-photon imaging and photostimulation with spatial light modulators," *Front. Neural Circ.* **2**, 5 (2008).
14. S. Zeng, X. Lv, C. Zhan, W. R. Chen, W. Xiong, S. L. Jacques, Q. Luo, "A spatio-temporally compensated acousto-optic scanner for two-photon microscopy providing large field of view." *Opt. Lett.* **31**, 1091 (2006).
15. Y. Shao, W. Qin, H. Liu, J. Qu, X. Peng, H. Niu, B. Z. Gao, "Ultrafast, large-field multiphotonmicroscopy based on an acousto-optic deflector and a spatial light modulator," *Opt. Lett.* **37**, 2532 (2012).
16. J. Qu, L. Liu, D. Chen, Z. Lin, G. Xu, B. Guo, H. Niu, "Temporally and spectrally resolved sampling imaging with a specially designed streak camera," *Opt. Lett.* **31**, 368 (2006).
17. D. N. Fittinghoff, J. A. Squier, "Time-decorrelated multifocal array for multiphoton microscopy and micromachining," *Opt. Lett.* **25**(16), 1213 (2000).
18. Y. Shao, W. Qin, H. Liu, J. Qu, X. Peng, H. Niu, B. Z. Gao, "Addressable multiregional and multifocal multiphoton microscopy based on a spatial light modulator," *J. Biomed. Opt.* **17**, 30505 (2012).
19. Y. Shao, W. Qin, H. Liu, J. Qu, X. Peng, H. Niu, B. Z. Gao, "Multifocal multiphoton microscopy based on a spatial light modulator," *Appl. Phys. B* **107**, 653 (2012).
20. G. Zhu, J. van Howe, M. Durst, W. Zipfel, C. Xu, "Simultaneous spatial and temporal focusing of femtosecond pulses," *Opt. Express* **13**, 2153 (2005).
21. J. Y. Yu, C. H. Kuo, D. B. Holland, Y. Chen, M. Ouyang, G. A. Blake, R. Zadoyan, C. L. Guo, "Wide-field optical sectioning for live-tissue imaging by plane-projection multiphoton microscopy," *J. Biomed. Opt.* **16**, 116009 (2011).
22. H. Dana, S. Shoham, "Remotely scanned multiphoton temporal focusing by axial grism scanning," *Opt. Lett.* **37**, 2913 (2012).
23. J. N. Yih, Y. Y. Hu, Y. D. Sie, L. C. Cheng, C. H. Lien, S. J. Chen, "Temporal focusing-based multiphoton excitation microscopy via digital micromirror device," *Opt. Lett.* **39**, 3134 (2014).
24. A. Bullen, S. S. Patel, P. Saggau, "High-Speed, Random-Access fluorescence microscopy: 1. High-Resolution optical recording with voltage-sensitive dyes and ion indicators," *Biophys. J.* **73**, 477 (1997).
25. P. J. Rodrigo, D. Palima, J. Gluckstad, "Accurate quantitative phase imaging using generalized phase contrast," *Opt. Express* **16**, 2740 (2008).
26. E. Papagiakoumou, F. Anselmi, A. Bgue, V. de Sars, J. Glückstad, E. Y. Isacoff, V. Emiliani, "Scanless two-photon excitation of channelrhodopsin-2," *Nat. Methods* **7**, 848 (2010).
27. J. M. Zaleskas *et al.*, "Contractile forces generated by articular chondrocytes in collagen–glycosaminoglycan matrices," *Biomaterials* **25**, 1299 (2004).
28. J. G. McNally, T. Karpova, J. Cooper, J. A. Conchello, "Three dimensional imaging by deconvolution microscopy," *Methods: A Companion to Methods in Enzymology* **19**, 373 (2016).